

Fully Coupled Atmosphere-Wave-Ocean Modeling for Hurricane Research and Prediction:

Results from CBLAST-Hurricane

Shuyi S. Chen^{1*}, Wei Zhao¹, Mark A. Donelan¹, James F. Price²,
Edward J. Walsh³, Thomas B. Sanford⁴, and Hendrik L. Tolman⁵

¹Rosenstiel School of Marine and Atmospheric Science

University of Miami, Miami, Florida

²Woods Hole Oceanographic Institution, Woods Hole, MA

³NASA/Goddard Space Flight Center, Wallops Island, Virginia

⁴Applied Physics Lab, University of Washington, Seattle, Washington

⁵Science Applications International Corporation/GSO at NOAA/NCEP, Camp Springs, MD

Submitted to BAMS

January 2006

*Corresponding Author: Dr. Shuyi S. Chen, RSMAS/University of Miami, Miami, FL 33149.

Email: schen@rsmas.miami.edu

ABSTRACT

Improving intensity forecast is the most important issue for hurricane prediction today. The lack of skill in forecasts of intensity may be attributed in part to deficiencies in the current prediction models: insufficient grid resolution, inadequate surface and boundary layer formulations, and the lack of full coupling to the ocean. The extreme high winds, intense rainfall, large ocean waves, and copious sea spray in hurricanes push the surface-exchange parameters for temperature, water vapor, and momentum into untested regimes. The Coupled Boundary Layer Air-Sea Transfer (CBLAST)-Hurricane program is aimed at developing improved coupling parameterizations, using the observations collected during the CBLAST-Hurricane field program, for the next generation hurricane research prediction models. Hurricane induced surface waves (that determine the surface stress) are highly asymmetric, which can affect storm structure and intensity significantly. The stress is supported mainly by waves in the wavelength range of 0.1-10 m, which are the unresolved “spectral tail” of present wave models. The CBLAST-Hurricane modeling team developed a wind-wave parameterization that includes effects of the wave spectral tail on the drag coefficient. This new parameterization has been implemented in a fully coupled atmosphere-wave-ocean model with 1-2 km resolution that can resolve many fine-scale features in the extreme high wind region of the eyewall. The coupling parameterization has been tested in a number of storms including Hurricane Frances (2004) that is one of the best observed storms during the CBLAST-Hurricane 2004 field program. Model simulations are evaluated with observations of directional wave spectra, sea surface temperature (SST), air-sea fluxes, profiles of atmospheric boundary layer, ocean temperature, salinity, and current from various in-situ, airborne, and satellite data during CBLAST-Hurricane. The fully coupled model with the new wind-wave parameterization gives an improved overall storm structure and intensity compared

with an uncoupled atmospheric model, and it produces a realistic surface pressure-wind relationship, which is especially sensitive to the treatment of surface stress.

1. Introduction

It has been recognized that the air-sea interaction plays an important role in hurricane intensity change (e.g., Emanuel 1986; 1995). However, one of the most difficult aspects is the complexity of the air-sea interaction on storm structure and evolution, which remains an unsolved problem. The extreme high winds and strong gradient zones of temperature and pressure are located in the inner core (eye and eyewall) of the hurricanes. To resolve the hurricane eye and eyewall structures, crucial in intensity forecasting, the horizontal resolution needs to be on the order of $\sim 1-2$ km. The air-sea interaction in the eyewall region is largely unknown with very few observations. While hurricanes draw energy from the ocean surface, they cool the ocean by wind-induced surface fluxes and vertical mixing. The enthalpy and momentum exchange coefficients under the high-wind conditions are difficult to determine. The stress is supported mainly by waves in the wavelength range of 0.1-10 m, which are unresolved by present wave models. Rapid increase in computer power and recent advance in technology in observations have made it possible for us to develop a strategy for the next generation of high-resolution hurricane prediction models. We begin by developing and examining key parameterizations including effects of the wave spectral tail on drag coefficients and subgrid-scale turbulence properties at 1-2 km resolution. This paper describes the results of a new wind-wave coupling parameterization based on the CBLAST observations. Coupled model simulation of Hurricanes Hurricane Frances (2004) is compared observations of surface wave spectra,

surface fluxes, and vertical profiles of atmospheric boundary layer and ocean mixed layer from recent hurricane field programs.

Hurricanes rarely reach their maximum potential intensity (MPI) (Emanuel 1986, 1995; Holland 1997). Many factors prevent storms from reaching MPI including environmental vertical wind shear, distribution of troposphere water vapor, hurricane internal dynamics, and air-sea interactions. The effect of the air-sea interactions, especially the wind-wave coupling under extreme high-wind conditions, on hurricane structure and intensity change is the focus of the CBLAST-Hurricane program (e.g., Black et al. 2006).

The upper-ocean response to hurricane forcing has been documented in some detail in modeling and observational studies (e.g., Price 1981, 1994; Shay and Elsberry 1987; Sanford et al. 1987; Bender and Ginis 2000; Shay et al. 2000). Hurricanes draw energy from the ocean, and hence they cool the ocean surface mixed layer (OML) and SST directly. In addition, the intense wind stress of a hurricane generates large amplitude near-inertial currents within the OML. The vertical shear associated with these currents causes significant vertical mixing which tends to deepen and cool the OML even more effectively than does the direct heat loss to the hurricane (Price, 1981; Shay *et al.* 1998). Upward vertical motion generated by the wind-driven currents (upwelling) may also enhance SST cooling by lifting the base of the OML and bringing cooler water closer to the sea surface. The amplitude of SST cooling due to a given hurricane thus depends in part upon the thermal stratification of the upper ocean, which is sometimes represented by an integrated heat content. Coupling to an ocean circulation model that includes a realistic thermal stratification, an appropriate parameterization of vertical mixing, and the possibility of upwelling is therefore necessary to ensure an accurate representation of the SST cooling.

Intensification of a hurricane depends also on two competing processes at the air-sea interface – the heat and moisture fluxes that fuel the storm and dissipation of kinetic energy to the ocean surface. Emanuel (1995) proposed that the storm intensity is largely controlled by the ratio of the air-sea enthalpy and momentum flux exchange coefficients, C_k/C_D . Using a simple axisymmetric model with idealized environmental conditions, Emanuel (1995) showed that this ratio needs to be equal or greater than one for hurricanes to intensify. As shown in many studies, although C_D is largely sea-state dependent (e.g., Toba et al. 1990; Donelan et al. 1993), C_k has relatively little sensitivity to sea-state (e.g., Geernaert et al. 1987). Recent laboratory experiments conducted at hurricane wind speeds have shown that C_D reaches a saturation point at high-wind speeds greater than about 33 m s^{-1} when flow separation begins to occur (Donelan et al. 2004); C_k , however, remains relatively constant. Recent airborne turbulence flux measurements from the CBLAST-Hurricane also support these laboratory results, indicating that C_k/C_D is less than one for intensifying storms, Hurricanes Fabian (2003) reported by Drennan et al. (2006).

This study aims to understand better the coupling between the upper ocean and SST, surface waves, and the atmosphere in hurricanes. A specific issue we emphasize here is the determination and parameterization of the air-sea momentum flux in conditions of extremely high and time-varying hurricane winds. We note that a related issue, the effects of sea spray on the air-sea exchange, may also be important (e.g., Fairall et al. 1994; Andreas and Emanuel 2001; Emanuel 2003), but the lack of comprehensive field data discourages us from attempting an explicit treatment of this complex problem at this time.

Three Atlantic hurricanes, Frances (2004), Floyd (1999) and Bonnie (1998), are examined in detail and simulated with both fully coupled and uncoupled models. Observations

from the 2004 CBLAST-Hurricane field program are used for model evaluation in Hurricane Frances.

2. Coupled modeling system

The fully coupled atmosphere-wave-ocean modeling system includes three model components, the atmospheric, surface wave, and ocean circulation models. Figure 1 shows a schematic of the coupled modeling system used in this study. The basic coupling parameters are listed among each of the model components in Fig. 1.

a. The atmospheric model

The atmospheric component of the coupled modeling system is the Fifth-Generation Penn State University/National Center for Atmospheric Research non-hydrostatic mesoscale model (MM5) (Grell et al. 1994, Dudhia 1993). To capture the long lifecycle of hurricanes and to resolve the inner-core structure, we developed a vortex-following nested grid that allows the model to be integrated for 5 days or longer at very high resolution (~1-2 km) in the inner most domain. With the automatic vortex-following nest system, mesh positions are not known in advance. It is not practical to pre-generate terrain and land use files prior to running a simulation. Accordingly, we have modified the MM5 nest initialization routine so that elevation and land use data are read and placed on the fine meshes each time they are initialized or moved. The vortex-following nested grid system is described in details in Tenerelli and Chen (2001) and Chen and Tenerelli (2006). We use four nests with 45, 15, 5, and 1.67 km grid spacing, respectively. The three inner domains move automatically with the storm. The domain sizes for each of the nests are 121x121, 121x121, and 151x151, respectively. There are 28 sigma-levels in the vertical with

about 9 levels within the atmospheric boundary layer. The model has been used to simulate Hurricane Bonnie (1998) (Rogers et al. 2003), Hurricane Georges (1998) (Cangialosi and Chen 2006), and Hurricane Floyd (1999) (Chen and Tenerelli 2006). These studies have shown that using 1.67 km grid spacing to resolve the inner-core (eye and eyewall) structure is a key in simulating hurricane evolution and intensity change.

We use an explicit moisture microphysics scheme and a slightly modified Kain-Fritsch (K-F) cumulus parameterization (Kain and Fritsch 1993) on the 45 and 15 km grids, and the explicit moisture scheme only on the 5 and 1.67 km grids. The microphysics scheme used is based on Tao and Simpson (1993). The inner core of hurricanes is simulated explicitly in cloud-resolving mode. Modifications to K-F parameterization include detraining of 30% hydrometeors to the resolvable grids and a higher vertical velocity threshold for initiation of convective clouds, which is more suitable for the tropical oceanic conditions. The Blackadar PBL scheme (Zhang and Anthes 1982) is used on all grids, but over water we include a modification based upon Garret (1992) in which we introduce different roughness scales for temperature z_t and moisture z_q . In the original formulation of the Blackadar scheme, the roughness scales for temperature and moisture are identical to that for momentum z_o , which was not appropriate since the physics governing momentum transfer at the surface are different from that governing temperature and moisture. In the uncoupled MM5 applications, the momentum roughness length over the open ocean is calculated from the Charnock relationship (Charnock 1955):

$$z_o = \alpha \frac{\tau}{\rho_a g} \quad (1)$$

where τ is the total stress, ρ_a is the air density, and α ($=0.0185$) is the Charnock parameter.

The National Center for Environmental Prediction (NCEP) global analysis fields (6 hourly and $1^\circ \times 1^\circ$) and the high-resolution (~ 9 km) AVHRR Pathfinder SST analysis (Chen, et al.,

2001) as well as the TMI-AMSR SST (~25 km) are used to initialize the uncoupled MM5 and provide continuous lateral and lower boundary conditions.

b. Ocean model

A three-dimensional, primitive equation, hydrostatic upper ocean model, 3DPWP, (Price et. al. 1994) is used to simulate the upper ocean current and temperature fields underneath the hurricane. The model domain is same with the outer domain of the atmospheric model with 15 km grid spacing. It has 30 vertical levels with grid spacing of 5-10 m for the top 20 levels and 20 m for the rest. It is initialized using observed and climatological temperature and salinity profiles. The temperature profile is blended from a selected, pre-storm Airborne eXpendable BathyThermograph (AXBT) observation from HRD aircraft missions and LEVITUS94 climatological temperature data for depths greater than sampled by AXBT observation. The salinity profile is entirely from LEVITUS94 climatology, since there is generally no in situ pre-storm observation available. At each time step of the ocean model, 10 minutes, the ocean model takes surface stress and heat and moisture fluxes from the atmospheric and wave models and steps ahead the ocean dynamics. On the same times, the ocean model passes back the SST anomaly (the difference between the initial and current SST) to the atmospheric model, and passes back the ocean surface current to the wave model. The simulations that utilize the ocean model to calculate the evolving SST will be referred to as 'A-O', meaning that both the atmosphere and the ocean evolve.

c. Surface wave model

A third-generation wave model, the WAVEWATCH III (WW3) (version 1.18) is used to simulate ocean surface waves in the Atmospheric-Ocean-Wave Coupling System. It was developed by Tolman (1991, 1999) for wind waves in slowly varying, unsteady and inhomogeneous ocean depths and currents. WW3 is extensively evaluated and validated with observations (Tolman et al. 2002). The wind waves are described by the action density wave spectrum $N(k, \theta, x, y, t)$. In this study, we use 25 frequency bands, logarithmically spaced from 0.0418 to 0.41 Hz at intervals of $\Delta f / f = 0.1$ and 48 directional bands (7.5° interval). The WW3 model domain is set to be about the same as the outer domain of MM5. The grid spacing is $1/6^\circ$ in both latitude and longitude. The water depth data used in the wave model is the 5' gridded elevation data from the National Geophysical Data Center. In the coupled system, the wave model inputs the surface wind and ocean surface current fields from the atmospheric and ocean models and outputs surface stress integrated from the wind-wave coupling parameterization discussed in detail in the next section. When the model includes this treatment of surface waves, the now fully coupled model will be referred to as 'A-W-O', meaning that the atmosphere, the surface waves and the ocean evolve.

3. Wind-wave coupling parameterization

The wave-induced stress contributes most of the total stress in high wind conditions (e.g., Donelan 1990). The coupling of the atmosphere through waves to the ocean is best served by a direct calculation of the evolution of the wave field and the concomitant energy and momentum transfer from wind to waves to upper oceanic layers. Existing third generation wave prediction models are unable to do this as their high wavenumber cut-off is about 0.63 m^{-1} or 10 m wavelength while most of the stress is supported by shorter waves. In WW3, the cut-off

frequency is set to $3f_{pi}$ (f_{pi} is the peak frequency of the dominant wave). In order to correct this short-coming a new wave and wind stress prediction model has been developed (Donelan, 2004) and is being tested against field and laboratory data with respect to its wave and stress prediction skill in rapidly changing wind conditions against direct measurements of wave spectra and Reynolds stress (Donelan et al. 2004). The new wind-wave parameterization calculates directional stress using surface wave directional spectra by parameterizing “spectral tails” (frequency $>$ cut-off frequency) unresolved by the current wave models is described here.

In most of the current coupled wind-wave models, roughness is treated as a scalar (Janssen 1991; Doyle 1995, 2002; Bao et al. 2000). However, the swirling winds in both extra-tropical and tropical cyclones are highly variable. The stress vector is not necessarily in the same direction as the local wind vector. The surface condition is mostly of the mixed wave-swell seas type. Instead of computing a scalar roughness from the total stress, we use a method of directional coupling of the wind and waves in a coupled atmosphere-wave-ocean model, in

which the tendencies of the wind affected by the wave stress are calculated as $\mathbf{u}_{\text{wave}} = \sqrt{\frac{\tau_x}{\rho_a C_D}}$

and $\mathbf{v}_{\text{wave}} = \sqrt{\frac{\tau_y}{\rho_a C_D}}$, where τ_x and τ_y are components of the stress vector due to the waves

(or “form drag”) that are computed from integral of momentum input to the spectrum:

$$\tau_x = g \frac{\rho_a}{\rho_w} \int_0^\infty \int_{-\pi}^\pi \frac{\gamma}{\omega} F(k, \vartheta) k_x k dk d\vartheta \quad (2)$$

$$\tau_y = g \frac{\rho_a}{\rho_w} \int_0^\infty \int_{-\pi}^\pi \frac{\gamma}{\omega} F(k, \vartheta) k_y k dk d\vartheta \quad (3)$$

The growth rate of each component from measurement of pressure-slope correlation

$$\frac{\gamma}{\omega} = A \frac{\rho_a}{\rho_w} \left[\frac{U_{(\pi/k)} \cos \theta}{C(k)} - 1 \right] \left| \frac{U_{(\pi/k)} \cos \theta}{C(k)} - 1 \right| \quad (4)$$

where U is the wind speed at $1/2$ wavelength height, C the phase speed, and A is the sheltering coefficient and, based on laboratory experiments, varies with wind speed, from 0.07-0.18. The spectrum of long waves is output from WAVEWATCH III. The spectrum of short waves from a fit to the tail of long waves is given below.

$$F(k, \mathcal{G}) = \alpha k^{-4} \sec h^2(\beta(\mathcal{G}_k)) \quad (5)$$

where α is a parameter adjusted for the spectral tail to fit the highest WW3 modeled wavenumbers and β is the argument of the spreading function for the short waves:

$$\beta = \frac{1.2}{\cos^{-1}(C/U)} \quad (6)$$

The skin stress is computed from the smooth law of the wall and taken to be in the wind direction. It is added to the wave (or form) drag to give the total stress vector.

Similar wind-wave coupling has been experimented with in Moon et al. (2004) by using the equilibrium spectrum formulation of Hara and Belcher (2004). However, the formulation is for mature waves, in which the effects of breaking waves are not included explicitly. They reached a very different conclusion than that of Kudryavtsev and Makin (2001) and Makin et al. (2002) when the breaking waves are included. The effect of breaking waves on wave-induced stress is particular important in high-wind conditions.

A recent experimental study by Donelan et al. (2004) indicates considerable structure in the aerodynamic drag versus wind speed. Figure 2 shows drag coefficients measured in the

laboratory with equivalent wind speed up to 60 m s^{-1} . One interesting feature shown in Donelan et al. (2004) is that the drag coefficient does not continue to increase with wind at high wind speed. It shows a remarkable “saturation” of the drag coefficient once the wind speed exceeds 33 m s^{-1} . Beyond this speed the surface simply does not become any rougher in an aerodynamic sense. In the range of wind speeds of 10 to 26 m s^{-1} these lab measurements parallel the open ocean measurements of Large and Pond (1981), but are a little lower. The measurements suggest aerodynamic roughness saturation beyond 10 m height wind speeds of 33 m s^{-1} . The saturation level for the drag coefficient is 0.0025 . This corresponds to a roughness length of 3.35 mm . An adjustment to agree with Large and Pond (1981) would suggest saturation at 0.0028 . Donelan et al. (2004) attributed a change in flow characteristics leading to saturated aerodynamic roughness, to a flow separation due to continuous wave breaking where the flow is unable to follow the wave crests and troughs, as shown in Reul et al. (1999). The saturation behavior of the drag coefficient is observed by Powell et al (2003) using wind profiles from dropsonde data in hurricanes.

4. Coupled simulations of three hurricanes

The CBLAST wind-wave coupling parameterization is tested in the fully coupled modeling system. To isolate the effects of the surface waves from that of upper-ocean circulation including SST, we conducted three separated model simulations for each storms, including the uncoupled MM5, coupled MM5-3DPWP or A-O, and fully coupled MM5-WW3-3DPWP or A-W-O. For the first time, very high-resolution hurricane simulations that capture the inner core structures of the Hurricanes Bonnie (1998), Floyd (1999), and Frances (2004) are used for simulations of hurricane ocean surface wave and upper ocean circulations.

a. Track and intensity

Hurricane tracks are mostly affected by the environmental steering flow. Figure 3 shows the observed and model simulated storm tracks for Hurricanes Frances, Floyd and Bonnie. The comparisons of the uncoupled, coupled A-O, and fully coupled A-W-O model simulated storm tracks indicate that the effects of the coupled wave and ocean are not large insofar as the storm track is concerned. While the uncoupled and coupled A-O model simulated tracks are almost the same, the fully coupled A-W-O model simulations improved tracks slightly in Hurricanes Frances and Bonnie.

In contrast, the effects of wave and ocean coupling on storm intensity are rather dramatic as shown in Fig. 4. The observed minimum sea-level pressure (MSLP) and maximum wind speed (MWS) from the NHC best track data are compared with the uncoupled and coupled model simulations. The uncoupled MM5, which uses a fixed pre-storm SST throughout of the simulations, overestimates MSLP (an integrated measure of the storm intensity) in all three storms. The coupled A-O, which includes the effect of SST cooling, due mostly to vertical mixing and secondarily to upwelling and direct cooling, produces a more realistic MSLP compared to the uncoupled MM5. However, both the uncoupled MM5 and coupled A-O simulations seem to underestimate MWS compared to the best track data in all three cases. The fully coupled A-W-O simulations are closest to the observed values. The discrepancy in MSLP and MWS in the uncoupled MM5 and coupled A-O simulations are evidently due to the lack of wind-wave coupling compared with the fully coupled A-W-O simulation as we will show later in this study.

b. Storm structures

To further examine the impact of the wave and ocean coupling, we compare the observed and simulated storm structures. Figure 5 shows observed radar reflectivity and the surface wind analysis (HWIND, see Power et al. 1998) in Hurricane Frances on 31 August 2004. The corresponding model simulated rainrate and surface wind speed at 1200 UTC on 31 August 2004 are shown in Fig. 6. Frances was a Category 4 storm with a MSLP of 945 hPa and maximum wind speed of 63 m s^{-1} . The eyewall is characterized with a narrow ring of strong wind and rainfall with a very steep gradient on both sides of the eyewall (Fig. 5). The fully coupled A-W-O simulation captures the high gradient zone and the asymmetries in the rainfall and surface wind field quite well (Fig. 6a), whereas the coupled A-O and uncoupled MM5 simulations depict a rather diffused eyewall (Fig. 6b and c). Another major difference between the fully coupled A-W-O and uncoupled MM5 simulations is in the outer rainband region, especially in the southeast side (or rear-left quadrant) of Frances, where rainfall was concentrated in a main band as observed by the airborne radar (Fig. 5a) and similarly in the A-W-O simulation (Fig. 6a). Both the A-O and uncoupled simulations tend to produce multiple rainbands in a broad region (Fig. 6b and c).

c. Upper ocean temperature and currents

Satellite observed post-Frances SST from the composite of GOES images and the TRMM TMI data are shown in Figs. 7a and b. The TMI SST is slightly warmer than that observed from GOES. The pre-storm TRMM TMI SST was used in the coupled modeling system at the initial time on August 27. The storm-induced cold wake in the SST is generally well simulated in the coupled model (Fig. 7c) compared with the satellite observations. The maximum cooling is to the

rear right of the storm center, as has been reported from other storms (e.g., Sanford et al. 1987). This right-track cooling bias is associated with the inertial motion in the upper-ocean current as simulated by the model (Fig. 7c).

Three EM-APEX floats were deployed near the Caribbean Islands before the passage of Hurricane Frances. The locations of the floats (1636, 1633, and 1634) are indicated in Fig. 7a. A detailed description of the autonomous vertically profiling T, S and V measuring EM-APEX floats and the data collected in Frances is given in Sanford (2004). Figure 8 shows the observed and model simulated upper-ocean temperature profiles in Hurricane Frances. The observed profile from pre-storm condition is used to initialize the ocean model. The cooling of the upper ocean in the wake of Frances is well reproduced by the coupled A-W-O model simulation.

Figure 9 shows the time-series of the observed upper-ocean temperature (T), salinity (S), and current (u, v) data from the EM-APEX float 1633 in pre-, during, and post-Hurricane Frances conditions. The corresponding upper-ocean properties simulated by the A-W-O model are shown in Fig. 10. The model simulates well the hurricane-induced near-inertial current, similar to that documented in Shay and Elsberry (1987) and Price et al. (1994).

d. Ocean surface waves

Model simulated ocean surface waves in hurricanes have been compared with observations from the NDBC buoys and directional wave spectrum from the NASA Scanning Altimeter (SRA) on board of the NOAA WP-3D aircraft during hurricane research flights. A detailed description of the airborne surface wave observations using SRA can be found in Wright et al. (2001). A recent study by Moon et al. (2003) compared the WW3 simulation of surface waves in Hurricane Bonnie (1998) with observations by Wright et al. (2001) and Walsh et al.

(2002). Using the coupled A-W-O, Zhao and Chen (2005) found that the model reproduces both the significant wave height (SWH) and wave periods near the US coasts before and during the hurricane passages over the 5-day forecast period compared with the NDBC buoy data, as well as the observed directional wave spectra around the hurricanes over the open water by SRA in both Bonnie (1998) and Floyd (1999).

The storm-induced surface wave field is highly complex and asymmetric around a hurricane. This is clearly evident in the A-W-O model simulated significant wave height (SWH) and wave length in Frances (Fig. 11). The highest surface waves, as measured by SWH, are usually observed in the right and front-right of the hurricane (Fig. 11a), similar to that in Bonnie (Wright et al. 2001). Frances is heading east-northeast at 1200 UTC on 31 August 2004. In a moving storm, the surface waves to the right of the storm center tends to grow into long and high waves because of the relatively long fetch than those to the left side of the storm (Fig. 11b). In contrast, the wind and the dominant waves are not aligned locally as shown in the directional wave spectra in Fig. 12, especially in the front-left where the wind and waves are from 90 to 180° out of phase. The fully coupled A-W-O model simulation of the directional wave spectra are compared with the SRA observations in Frances on 1 September 2004 (Fig. 12). The directional wave spectra observed by the airborne SRA in Hurricane Frances show features that are similar to other major hurricanes over the open ocean (e.g., Wright et al 2001). In the rear-left quadrant of the hurricane, the directional wave spectrum is most complex with multiple spectrum peaks in both down-wind and cross-wind directions. The dominant wavelength is shorter than in the front-right quadrant (Fig. 12).

e. Air-sea exchange coefficients

Figure 13 shows the drag coefficient, C_D , and enthalpy exchange coefficient, C_k , in Hurricane Frances from the uncoupled and fully coupled A-W-O simulations. It is important to note that the C_D is explicitly wave-dependent in the coupled model, which can be seen in Fig. 13, as the front quadrants of a hurricane are “smoother” than the rear quadrants where the wavelength is shorter. The uncoupled simulation, in contrast, has the largest C_D value (a function of wind speed through the Charnock relationship) in the front-right quadrant. The enthalpy exchange coefficient, C_k , is calculated using the roughness length for the heat and moisture fluxes, z_t and z_q , in both coupled and uncoupled simulations. There is a significant spatial variability of C_D in a hurricane, which is due mostly to the variation in surface waves in the fully coupled A-W-O (Fig. 13a), whereas to surface wind speed in the uncoupled MM5 simulations (Fig. 13b). However, C_k varies only slightly from $1.1-1.2 \times 10^{-3}$. Observations of C_k and C_D in high wind conditions are difficult to obtain. Results from Liu et al. (1979) are representative of wind speeds less than 20 m s^{-1} . Recent CBLAST-Hurricane observations by Drennan et al. (2006) have obtained direct measurements in wind speeds up to 32 m s^{-1} in Hurricane Fabian (2003). They found that C_k changes little with wind speed and remains on average at 1.1×10^{-3} . The ratio, C_k / C_D , therefore, varies spatially in a hurricane due mostly to the variation in C_D .

The ratio of the exchange coefficients vary from 1 in the outermost part of the storm where wind speeds are less than 20 m s^{-1} to 0.4 in the eyewall region where the wind speed reaches $50-60 \text{ m s}^{-1}$ in the fully coupled A-W-O simulation (Fig. 13). In the uncoupled simulation the ratio is 0.3 or less in the eyewall region, similar to the results reported by Bao et al. (2002). Hurricane Frances continues to intensify even while the ratio was less than one, especially near the inner core region of the storm in these simulations. The CBLAST observations support that C_k / C_D may be less than 0.75 (e.g., Black et al. 2006). This difference

between the coupled modeling results and that of Emanuel (1995) using an axisymmetric hurricane model with a bulk ABL parameterization is that gradient winds are used in Emanuel's calculation. Furthermore the depth of the ABL in hurricanes decreases toward the storm center, which is resolved in MM5, but not in the bulk ABL in Emanuel (1995). The gradient wind at the top of the ABL, as in Emanuel's model, is not representative of the surface wind.

f. Surface heat fluxes

The corresponding surface heat (sensible + latent) fluxes from the model simulations are shown in Fig. 14. The combined effect of the atmosphere-wave-ocean coupling produces an increased asymmetry in the air-sea fluxes. The uncoupled MM5 simulation produced a more symmetric heat flux (Fig. 14c) compared to that of coupled model simulation (Figs. 14a and b). A similar asymmetry in surface heat flux has also been observed during the CBLAST-Hurricane field programs in 2003 and 2004 (Black et al. 2006; Drennan et al. 2006). The storm-induced upper ocean cooling in the right-rear quadrant not only contributes to the asymmetry, but also reduces the overall surface heat fluxes in Frances from the inner core to the outer rainband regions as a result of reduced storm intensity (Figs. 14b and c). The effect of the wind-wave coupling in the fully coupled A-W-O simulation seems to increase the latent heat flux in the eyewall region where the drag coefficient remains nearly constant as wind increases (Figs. 13a and c). It also increases the heat fluxes in the front-right quadrant where the longest wavelength and relatively small value in C_D are located. The enhanced surface wind in the fully coupled A-W-O, as a result of the sea-state-dependent stress that is reduced in extreme high winds compared with the uncoupled MM5 and coupled A-O, contributes to the increased surface heat

(mostly latent) flux in the eyewall and front-right quadrant of Hurricane Frances (Fig. 14) and similarly in Hurricanes Floyd and Bonnie.

g. Pressure-wind relationship

The pressure and wind speed relationship of a hurricane is one of the most complex and difficult parameters to predict, because it is quite sensitive to the details of the treatment of surface roughness and momentum flux. The fully coupled model with the new wind-wave parameterization improves the surface pressure-wind relationship in all three hurricanes, Frances, Floyd, and Bonnie, compared with the observations of Landsea et al. (2004) shown in Fig. 15. The uncoupled atmospheric model over-predicts the MSLP by 10-30 hPa, and under-predicts the MWS by 10-15 m s^{-1} , while the A-O coupled model improves the MSLP but still under-predicts the surface wind.

This last result is perhaps the most interesting and important outcome of the coupled model simulations using the CBLAST wind-wave coupling parameterization. It reveals that the full wind-wave coupling presented in Section 3 produces a more realistic pressure-wind relationship in hurricanes than does the empirical Charnock relationship (Charnock 1955) used in the uncoupled models. It has an important implication for the application of future hurricane intensity forecasting.

5. Conclusions

The CBLAST wind-wave parameterization has been tested in a fully coupled atmosphere-wave-ocean model by simulating the tracks, structure, and intensity of three Atlantic Hurricanes. Observations from the CBLAST-Hurricane field program provided a unique data set

to evaluate and validate fully coupled models. The high-resolution, fully coupled model is capable of capturing the complex hurricane structure and intensity change in Hurricanes Bonnie (1998), Floyd (1999), and Frances (2004). The coupling to the ocean circulation model improves the storm intensity by including the storm-induced cooling in the upper ocean and SST, whereas the uncoupled atmosphere model with a constant SST over-intensifies the storms. However, without coupling to the surface waves explicitly, both the uncoupled atmospheric model and the coupled atmosphere-ocean model underestimate the surface wind speed, even though the MSLP of especially the A-O coupled model is close to the observed values. The full coupling with the CBLAST wave-wind parameterization clearly improves the model simulated wind-pressure relationship that is a key issue in hurricane intensity forecasting.

Acknowledgement. The CBLAST-Hurricane is a research program supported by a Departmental Research Initiative (DRI) at the Office of Naval Research (ONR). NOAA AOC provided critical support in operations of the NOAA WP-3D aircraft during the CBLAST-Hurricane field program in 2003 and 2004. Researchers in the CBLAST-Hurricane observation team lead by Dr. Peter Black are acknowledged for their input and discussions during the course of this study. The research is supported by the ONR research grants N00014-01-1-0156, N00014-04-1-0109, and SBIR for the EM-APEX development and deployment.

References

Andreas, E. L. and K. Emanuel, 2001: Effects of sea spray on tropical cyclone intensity. *J. Atmos. Sci.*, **58**, 3741-3751.

- Bao, J.-W., S. A., Michelson, and J. M. Wilczak, 2002: Sensitivity of numerical simulations to parameterizations of roughness for surface heat fluxes at high winds over the sea. *Mon. Wea. Rev.*, **130**, 1926-1932.
- Bao, J.-W., J. M. Wilczak, and J.-K. Choi, 2000: Numerical simulations of air-sea interaction under high wind conditions using a coupled model: A study of hurricane development. *Mon. Wea. Rev.*, **128**, 2190-2210.
- Bender, M. A., and I. Ginis, 2000: Real-case simulations of hurricane-ocean interaction using a high-resolution coupled model: Effects on hurricane intensity. *Mon. Wea. Rev.*, **128**, 917-946.
- Black, P. G., Eric A. D'Asaro, J. R. French, and W. M. Drennan, 2006: Air-Sea Exchange in Hurricanes: Synthesis of Observations from the Coupled Boundary Layer Air-Sea Transfer Experiment. *Bull. Amer. Meteor. Soc.*, submitted.
- Charnock, H., 1955: Wind stress on a water surface. *Quart. J. Roy. Meteor. Soc.*, **81**, 639-640.
- Chen, S. S., J. E. Tenerelli, W. Zhao, and M. A. Donelan, 2004: Coupled atmosphere-wave-ocean parameterizations for high winds. *Preprints, 13th Conference on Interactions of the Sea and the Atmosphere, 9-13 August 2004, Portland, Maine, AMS.*
- Chen, S. S., and J. E. Tenerelli, 2006: Simulation of hurricane lifecycle and inner-core structure using a vortex-following mesh refinement: Sensitivity to model grid resolution. *Mon. Wea. Rev.*, submitted.

- Chen, S. S., W. Drennan, H.-J. Xue, and P. Chu, 2005: Coastal atmosphere-wave-ocean coupling, *Coupled Coastal Wind-Wave-Current Dynamics*, SCOR, Graig et al. Ed.
- Chen, S. S., W. Zhao, J. E. Tenerelli, R. H. Evans, and V. Halliwell, 2001: Impact of the AVHRR sea surface temperature on atmospheric forcing in the Japan/East Sea, *Geophys. Res. Lett.*, **28**, 4539-4542.
- Donelan, M. A., Dobson, F. W., Smith, S. D., Anderson, R. J. 1993: On the Dependence of Sea Surface Roughness on Wave Development. *J. Phys. Oceanogr.*, 23, 2143-2152.
- Donelan, M. A., B. K. Haus, N. Reul, W. J. Plant, M. Stiassnie, H. C. Graber, O. B. Brown, E. S. Saltzman, 2004: On the limiting aerodynamic roughness of the ocean in very strong winds, *Geophys. Res. Lett.*, **31**, 4539-4542.
- Doyle, J. D., 1995: Coupled ocean wave/atmosphere mesoscale model simulations of cyclogenesis. *Tellus*, **47A**, 766-788.
- Doyle, J. D., 2002: Coupled atmosphere-ocean wave simulations under high-wind conditions. *Mon. Wea. Rev.*, **130**, 3087-3099.
- Drennan, W. M., J. Zhang, J. R. French, C. McCormick, P. Black, 2006: Turbulence fluxes in the hurricane boundary. Part II: Latent heat fluxes. *J. Atmos. Sci.*, to be submitted.
- Emanuel, K., 1986: An air-sea interaction theory for tropical cyclones. Part I: Steady-state maintenance. *J. Atmos. Sci.*, **43**, 585-604.
- Emanuel, K., 1995: Sensitivity of tropical cyclones to surface exchange coefficients and a revised steady-state model incorporating eye dynamics. *J. Atmos. Sci.*, **52**, 3969-3976.
- Emanuel, K., 2003: A similarity hypothesis for air-sea exchange at extreme wind speeds. *J. Atmos. Sci.*, **60**, 1420-1428.

- Fairall, C. W., J. D. Kepert, and G. J. Holland, 1994: The effect of sea spray on surface energy transport over the ocean. *Global Atmos. Ocean Syst.*, **2**, 154-160.
- Garratt, J. R., 1992: The atmosphere boundary layer. *Cambridge University Press*, 316 pp.
- Hara, T., and S. E. Belcher, 2004: Wind profile and drag coefficient over mature ocean wave spectra. *J. Physical Ocean.*, **34**, 2345-2358.
- Large, W.G. and S. Pond, 1981: Open ocean momentum flux measurements in moderate to strong winds. *J. Phys. Oceanogr.*, **11**, 324-336.
- Landsea, C. W., C. Anderson, N. Charles, G. Clark, J. Dunion, J. Fernandez-Partagas, P. Hungerford, C. Neumann, and M. Zimmer, 2004: The Atlantic hurricane database re-analysis project: Documentation for the 1851-1910 alterations and additions to the HURDAT database. *Hurricanes and Typhoons: Past, Present and Future*, R. J. Murname and K.-B. Liu, Eds., Columbia University Press, 177-221.
- Kudryavtsev, V. N., and V. K. Makin, 2001: The impact of air-flow separation on the drag of the sea surface. *Bound.- Layer Meteor.*, **98**, 155-171.
- Makin, V. K., and V. N. Kudryavtsev, 2002: Impact of dominant waves on sea drag. *Bound.- Layer Meteor.*, **103**, 83-99.
- Moon, I.-J., I. Ginis, T. Hara, H. L. Tolman, C. W. Wright and E. J. Walsh, 2003: Numerical simulation of sea surface directional wave spectra under hurricane wind forcing. *J. Phys. Oceanogr.*, **33**, 1680-1706.
- Moon, I.-J., T. Hara, I. Ginis, S. E. Belcher, and H. L. Tolman, 2004: Effect of surface waves on air-sea momentum exchange. Part I: Effect of mature and growing seas. *J. Atmos. Sci.*, **61**, 2321-2333.
- Price, J. F., 1981: Upper ocean response to a hurricane. *J. Phys. Oceanogr.*, **11**, 153-175.

- Price, J. F., T. B. Sanford, and G. Z. Forristall, 1994: Forced Stage Response to a Moving Hurricane. *J. Phys. Oceanogr.*, **24**, 233–260.
- Powell, M. D., S. H. Houston, L. R. Amat, N. Morisseau-Leroy, 1998: The HRD real-time hurricane wind analysis system. *J. Wind Engineer. Ind. Aerody.*, **77&78**, 53-64.
- Powell, M. D., P. J. Vickery, and T.A. Reinhold, 2003: Reduced drag coefficient for high wind speeds in tropical cyclones. *Nature*, **422**, 279-283.
- Reul, N., H. Branger, and J.-P. Giovanangeli, Air flow separation over unsteady breaking waves. *Phys. Fluids*, **11** (7), 1959-1961, 1999.
- Rogers, R., S. S. Chen, J. E. Tenerelli, and H. E. Willoughby, 2003: A numerical study of the impact of vertical shear on the distribution of rainfall in Hurricane Bonnie (1998), *Mon. Wea. Rev.*, **131**, 1577-1599.
- Sanford, T. B., 2004: Preliminary results and interpretations from EM-APEX floats deployed in Hurricane Frances, September 2004. (A Note from the CBLAST-Hurricane 2004 field program.)
- Sanford, T. B., P. G. Black, J. Haustein, J. W. Fenney, G. Z. Forristall and J. F. Price, 1987: Ocean response to hurricanes. Part I: Observations. *J. Phys. Oceanogr.*, **17**, 2065-2083.
- Shay, L. K. and R. L. Elsberry, 1987: Near-inertial ocean current response to Hurricane Frederic. *J. Phys. Oceanogr.*, **17**, 1249-1269.
- Shay, L. K., G. J. Goni, F. D. Marks, J. J. Cione, and P. G. Black, 2000: Effects of a warm oceanic feature on Hurricane Opal. *Mon. Wea. Rev.*, **128**, 1366-1383.
- Tenerelli, J. E., S. S. Chen, 2001: High-resolution simulation of Hurricane Floyd (1999) using MM5 with a vortex-following mesh refinement. *Preprints, 18th Conference on Weather*

- Analysis and Forecasting/14th Conference on Numerical Weather Prediction, 30 July-2 August 2001, Ft. Lauderdale, Florida, AMS, J54-J56.*
- Tolman, H. L. 1991: A Third-Generation Model for Wind Waves on Slowly Varying, Unsteady, and Inhomogeneous Depths and Currents. *J. Phys. Oceanogr.*, 21, 782-797.
- Tolman, H. L., 1999: User manual and system documentation of WAVEWATCH-III version 1.18. NOAA / NWS / NCEP / OMB Technical Note Nr. **166**, 110 pp.
- Tolman, H. L., B. Balasubramanian, L. D. Burroughs, D. V. Chalikov, Y. Y. Chao, H. S. Chen, and V. M. Gerald, 2002: Development and implementation of wind generated ocean surface wave models at NCEP. *Weather and Forecasting*, **17**, 311-333
- Walsh, E. J., and Coauthors, 2002: Hurricane directional wave spectrum spatial variation at landfall. *J. Phys. Oceanogr.*, 32, 1667-1684.
- Wright, C. W., and Coauthors, 2001: Hurricane directional wave spectrum spatial variation in the open ocean. *J. Phys. Oceanogr.*, 31, 2472-2488.
- Zhao, W., and S. S. Chen, 2004: Upper Ocean Response and Feedback to 2002 Hurricanes Isidore and Lili in Tandem. *Proceedings of 26th Conference on Hurricanes and Tropical Meteorology, Miami, 3-7 May 2004, AMS*
- Zhao, W., and S. S. Chen, 2005: A Coupled Atmosphere-Wave-Ocean Framework for High-Resolution Modeling of Tropical Cyclones and Coastal Storms, *The WRF and MM5 User Workshop, Boulder, 26-30 June 2005, NCAR note.*

Figure Captions

Figure 1. Schematics of a fully coupled atmosphere-wave-ocean modeling system with the component atmosphere, surface wave, and ocean circulation models, as well as the coupling parameters among each of the components.

Figure 2. Laboratory measurements of the neutral stability drag coefficient by profile, eddy correlation (“Reynolds”) and momentum budget methods. The drag coefficient refers to the wind speed measured at the standard anemometer height of 10 m. The frequently cited drag coefficient formula of Large and Pond [1981] is also shown. This was derived from field measurements. (Adapted from Donelan et al. 2004. Note that “This paper” in the label refers to Donelan et al. 2004.)

Figure 3. Observed (the NHC best track in black) and simulated storm tracks from the fully coupled atmosphere-wave-ocean model (red), coupled atmosphere-ocean model (green), and uncoupled atmosphere model (blue), for Hurricanes Frances (circles), Floyd (triangles), and Bonnie (squares).

Figure 4. Observed (the NHC best track in black) and simulated MSLP (dashed lines) and maximum wind speed (solid lines) from the fully coupled atmosphere-wave-ocean model (red), coupled atmosphere-ocean model (green), and uncoupled atmosphere model (blue), for Hurricanes Frances (a), Floyd (b), and Bonnie (c).

Figure 5. (a) Observed radar reflectivity composite from 1711-1731 UTC and (b) HWind at 1930 UTC from the NOAA WD-P3 aircraft in Hurricane Frances on 31 August 2004.

Figure 6. Simulated rainrate (color, mm h^{-1}) and surface wind speed (black contour with 10 m s^{-1} interval) in Hurricane Frances at 1200 UTC 31 August 2004 from (a) fully coupled

atmosphere-wave-ocean, (b) coupled atmosphere-ocean, and (c) uncoupled atmosphere models.

Figure 7. Observed SST from (a) the GOES and (b) the TRMM TMI-AMSRE daily composite on 5 September 2004, respectively, and (c) fully coupled model simulated SST and ocean surface current in Hurricane Frances at 1200 UTC 4 September 2004. Storm tracks are overlaid on each of the SST maps. The red stars in (a) indicate the locations of the EM-APEX floats: 1636 (on the storm track), 1633 and 1634 (50 and 100 km away from the storm center, respectively).

Figure 8. Ocean temperature profiles observed from the EM-APEX float 1633 prior to Hurricane Frances at about 2000 UTC on 31 August (black) and after the hurricane passage at 1800 UTC on 1 September 2004 (blue) as well as the corresponding temperature profile simulated by the fully coupled model (red).

Figure 9. Observed upper-ocean temperature ($^{\circ}\text{C}$) (a), salinity (psu) (b), and current (u, v , in m s^{-1}) (c and d) from the EM-APEX float 1633. Day 0 marks the passage of Hurricane Frances at the float at 1200 UTC on 1 September 2004.

Figure 10. Same as in Fig. 9, except for the fully coupled model simulated fields.

Figure 11. A-W-O model simulated (a) SWH (color, m) and wave propagation direction (white vectors) and (b) mean wavelength (color, m) and surface wind (black vectors) at 1200 UTC on 31 August 2004. The black “+” indicates the storm center of Hurricane Frances. The arrow in the lower left corner indicates the direction of the storm motion.

Figure 12. Observed and model simulated directional wave spectra in Hurricane Frances. The top four panels are from the SRA data in the front-left, front-right, rear-left, and rear-right quadrants from 1640-2011 UTC on 1 September 2004. The bottom four panels are the

corresponding directional wave spectra from the fully coupled model simulation of Frances.

Figure 13. (a) and (b) The fully coupled and uncoupled model simulated drag coefficient in Hurricane Frances at 1200 UTC 31 August 2004. The white lines indicate the four quadrants relative to the storm motion as shown by the white vectors. (c) and (d) Corresponding scatter plots of the drag coefficients and enthalpy exchange coefficient. Data from the four quadrants are shown in different colors as indicated at the top right corner. Similarly the black vectors indicate the direction of the storm motion.

Figure 14. Simulated enthalpy (sensible+latent) flux (color, W m^{-2}) and surface wind (vector) in Hurricane Frances at 1200 UTC 31 August 2004 from (a) fully coupled atmosphere-wave-ocean, (b) coupled atmosphere-ocean, and (c) uncoupled atmosphere models.

Figure 15. Observed (the NHC best track data, black circles) and simulated pressure-wind relationship from the fully coupled atmosphere-wave-ocean model (red), the coupled atmosphere-ocean model (green), and the uncoupled atmosphere model (blue) for Hurricanes Frances (a), Floyd (b), and Bonnie (c).

Coupled Atmosphere-Wave-Ocean Modeling System

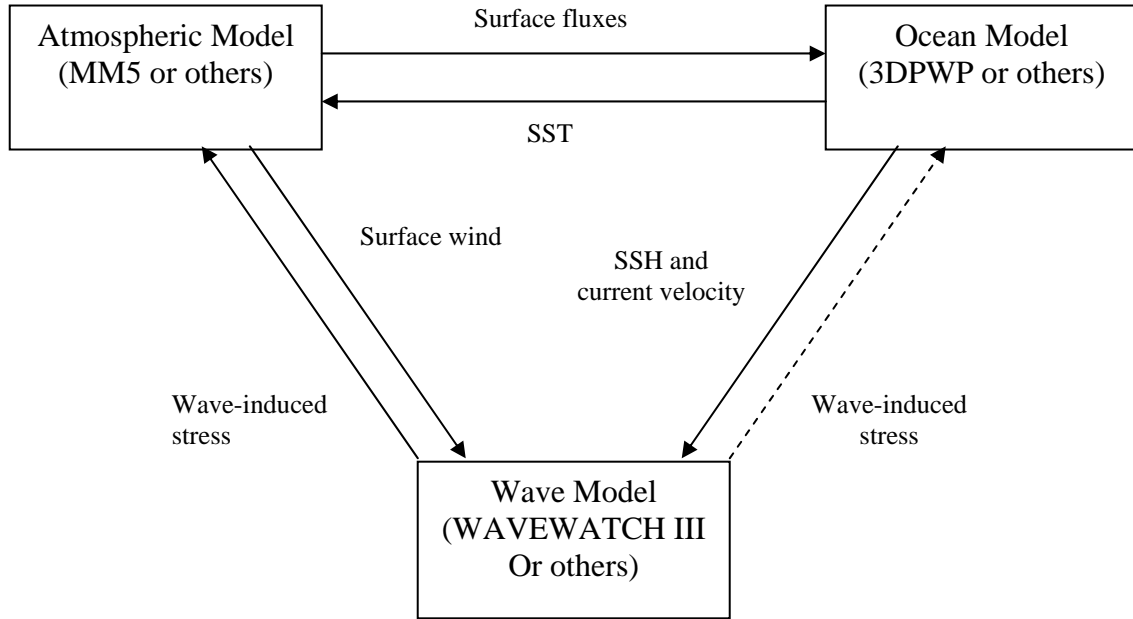


Figure 1. Schematics of a fully coupled atmosphere-wave-ocean modeling system with the component atmosphere, surface wave, and ocean circulation models, as well as the coupling parameters among each of the components.

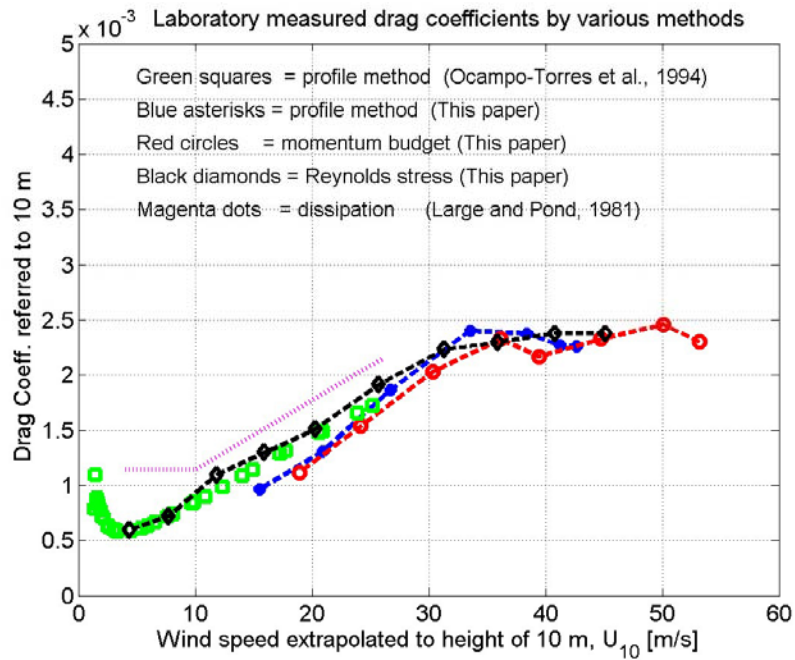


Figure 2. Laboratory measurements of the neutral stability drag coefficient by profile, eddy correlation (“Reynolds”) and momentum budget methods. The drag coefficient refers to the wind speed measured at the standard anemometer height of 10 m. The frequently cited drag coefficient formula of Large and Pond [1981] is also shown. This was derived from field measurements. (Adapted from Donelan et al. 2004. Note that “This paper” in the label refers to Donelan et al. 2004.)

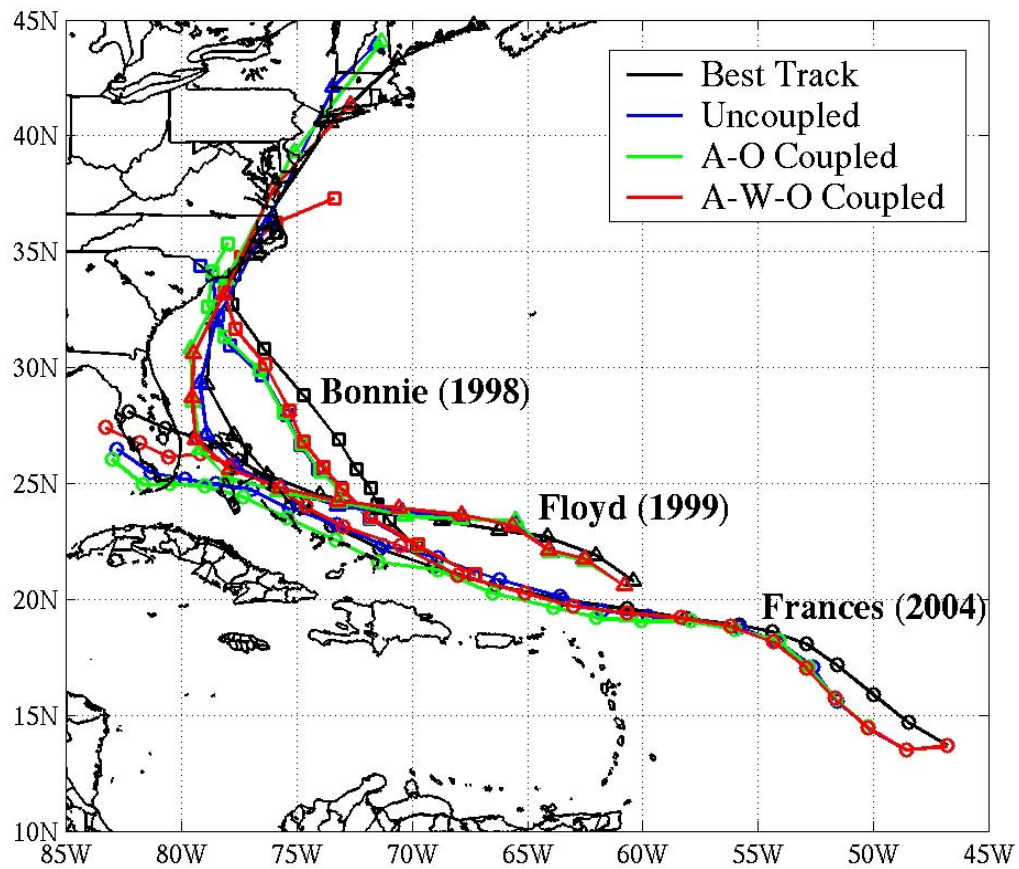


Figure 3. Observed (the NHC best track in black) and simulated storm tracks from the fully coupled atmosphere-wave-ocean model (red), coupled atmosphere-ocean model (green), and uncoupled atmosphere model (blue), for Hurricanes Frances (circles), Floyd (triangles), and Bonnie (squares).

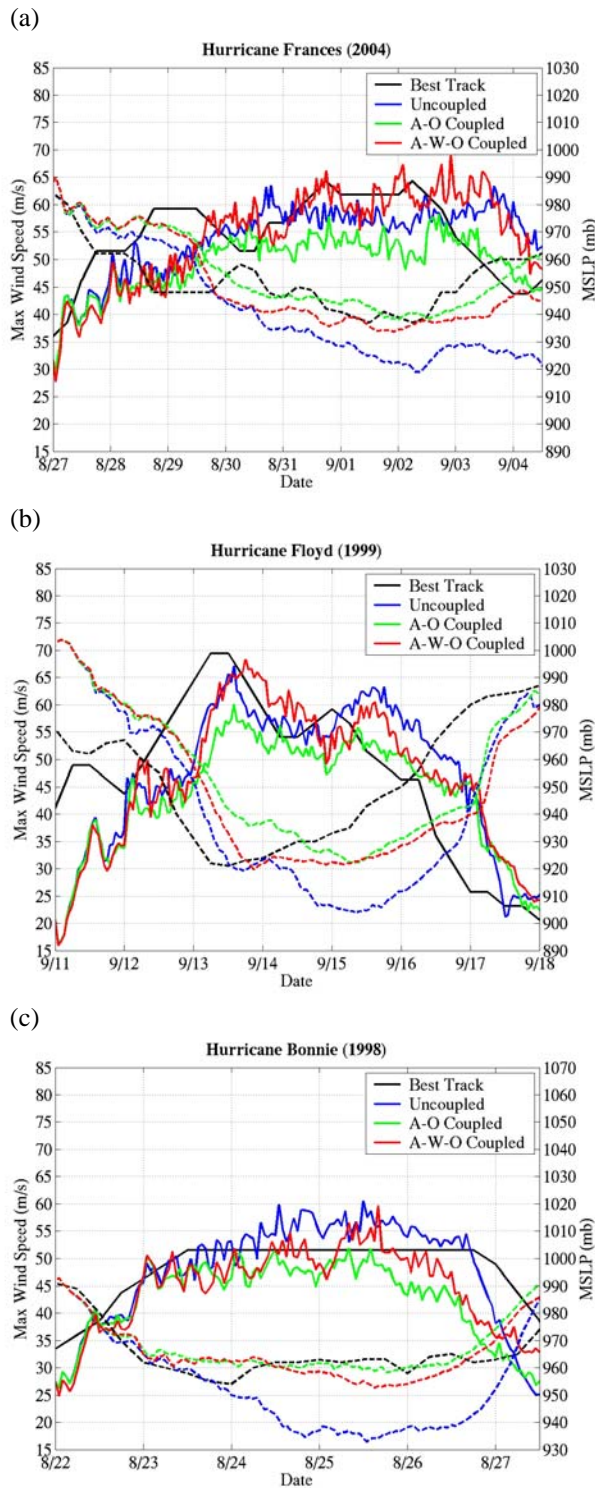
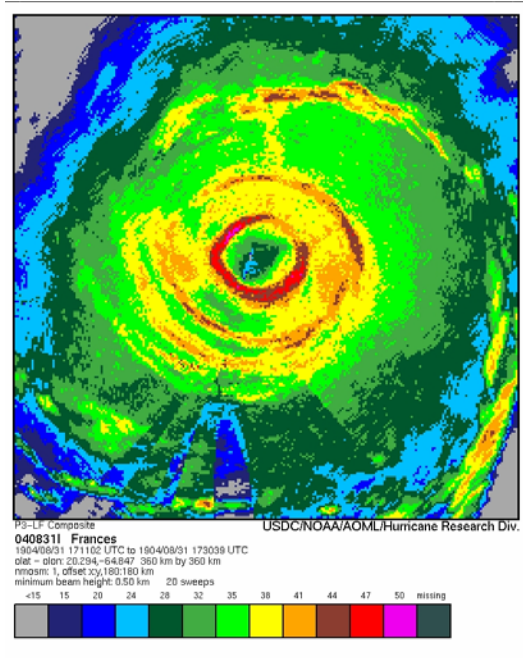


Figure 4. Observed (the NHC best track in black) and simulated MSLP (dashed lines) and maximum wind speed (solid lines) from the fully coupled atmosphere-wave-ocean model (red), coupled atmosphere-ocean model (green), and uncoupled atmosphere model (blue), for Hurricanes Frances (a), Floyd (b), and Bonnie (c).

(a)

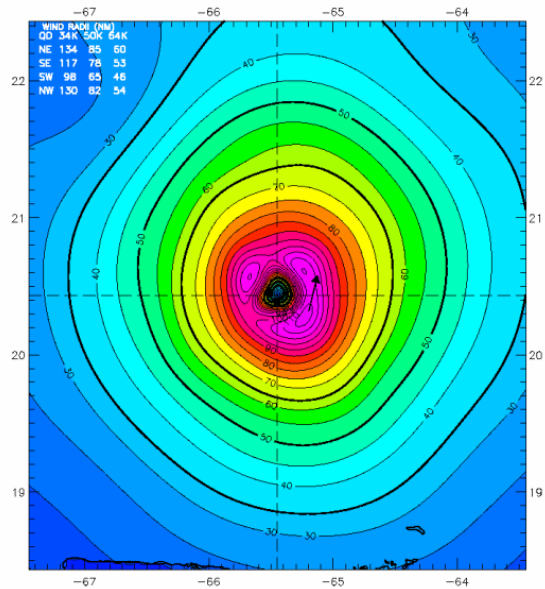


(b)

Hurricane Frances 1930 UTC 31 Aug 2004

Max 1-min sustained surface winds (kt) for marine exposure

Analysis based on GPSSONDE_WL150 from 1907 - 1907 z; DRIFTING_BUOY from 1600 - 1600 z;
SFM43 from 1930 - 1930 z; ASOS_LD_TO from 1356 - 1856 z;
GPSSONDE_MBL from 1907 - 1907 z; GPSSONDE_SFC from 1907 - 1907 z;
GOES from 1559 - 1559 z;
1930 z position extrapolated from 1923 z User wind center using 280 deg @ 15 kts; mslp = 940.0 mb



Observed Max. Surface Wind: 118 kts, 16 nm SE of center based on 1927 z SFMR43 sfc measurement
Analyzed Max. Wind: 118 kts, 16 nm SE of center
Experimental research product of:
NOAA / AOML / Hurricane Research Division

Figure 5. (a) Observed radar reflectivity composite from 1711-1731 UTC and (b) HWind at 1930 UTC from the NOAA WD-P3 aircraft in Hurricane Frances on 31 August 2004.

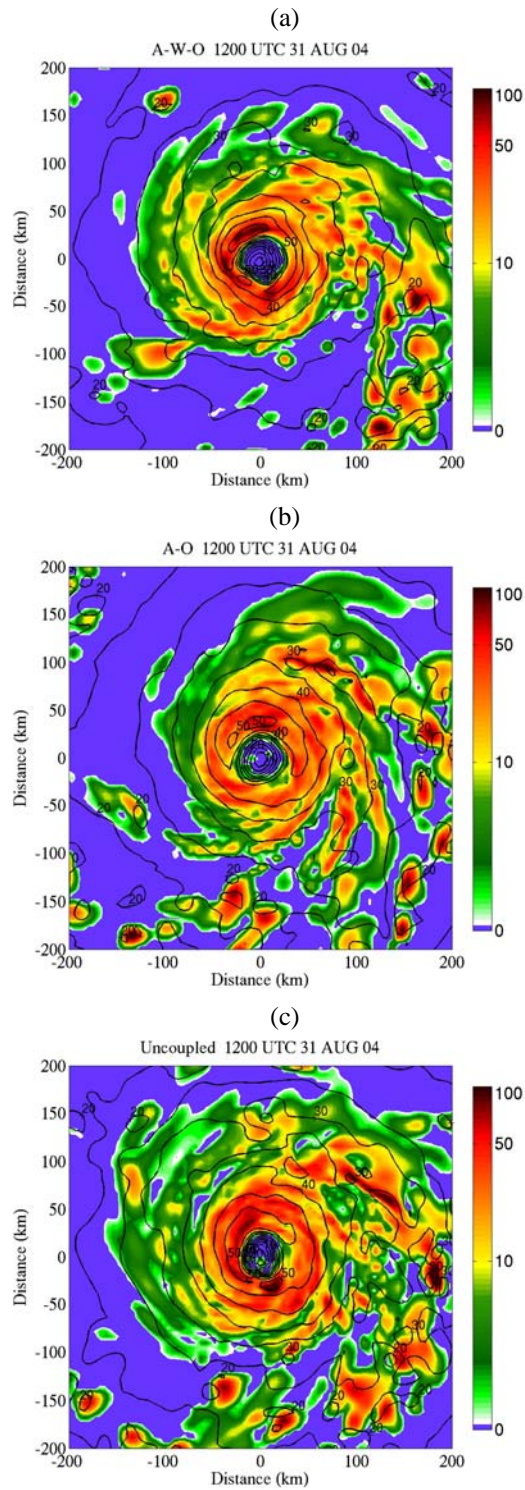


Figure 6. Simulated rainrate (color, mm h^{-1}) and surface wind speed (black contour with 10 m s^{-1} interval) in Hurricane Frances at 1200 UTC 31 August 2004 from (a) fully coupled atmosphere-wave-ocean, (b) coupled atmosphere-ocean, and (c) uncoupled atmosphere models.

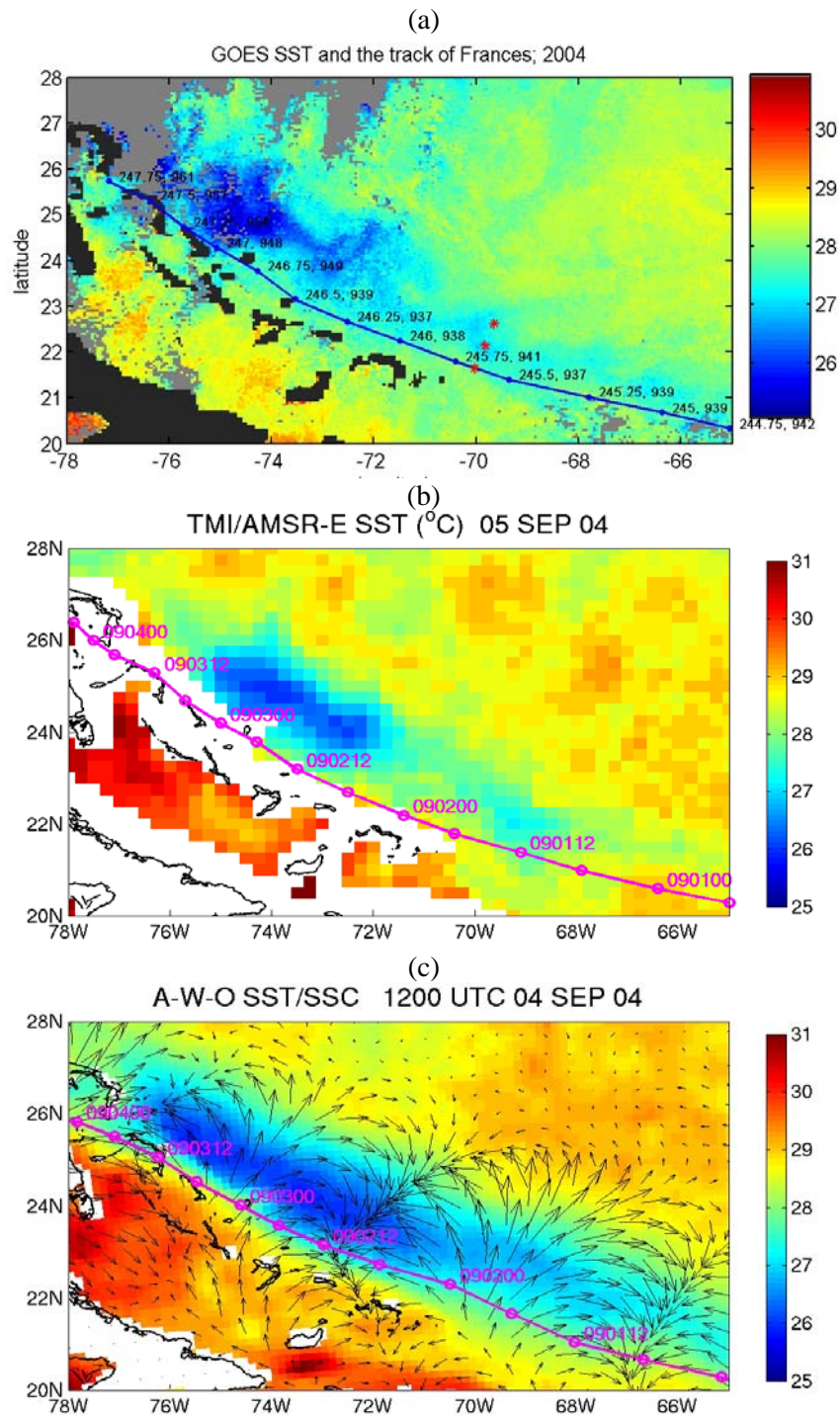


Figure 7. Observed SST from (a) the GOES and (b) the TRMM TMI-AMSRE daily composite on 5 September 2004, respectively, and (c) fully coupled model simulated SST and ocean surface current in Hurricane Frances at 1200 UTC 4 September 2004. Storm tracks are overlaid on each of the SST maps. The red stars in (a) indicate the locations of the EM-APEX floats: 1636 (on the storm track), 1633 and 1634 (50 and 100 km away from the storm center, respectively).

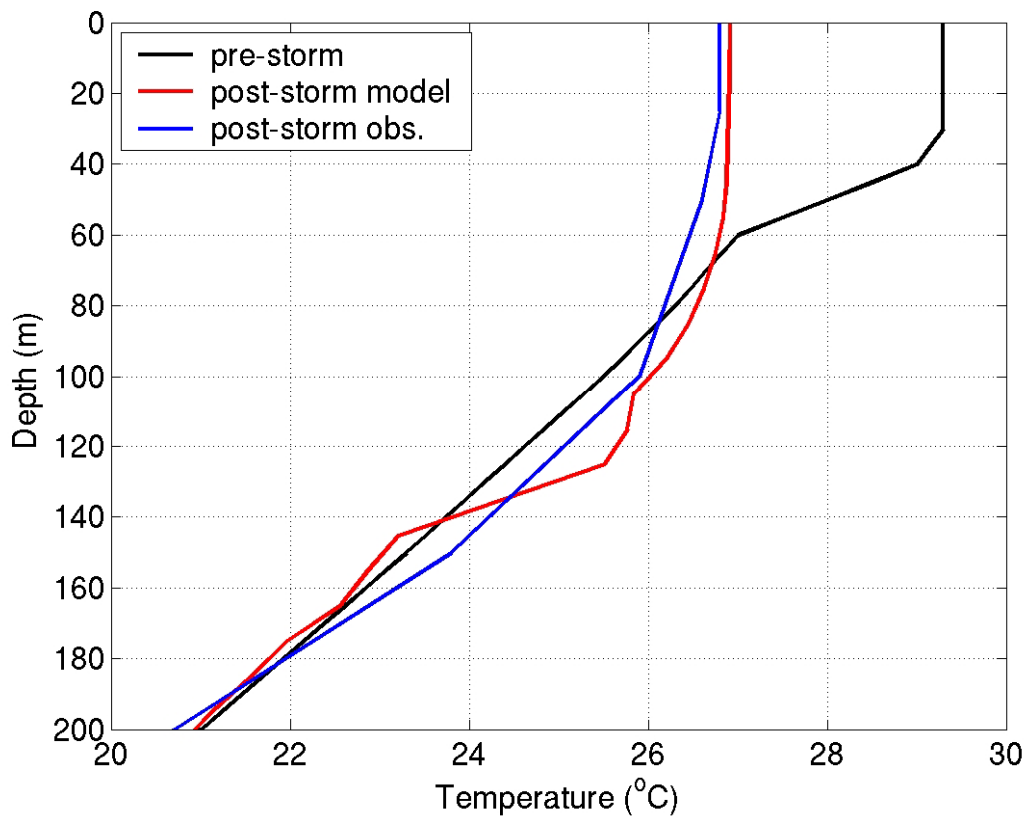


Figure 8. Ocean temperature profiles observed from the EM-APEX float 1633 prior to Hurricane Frances at about 2000 UTC on 31 August (black) and after the hurricane passage at 1800 UTC on 1 September 2004 (blue) as well as the corresponding temperature profile simulated by the fully coupled model (red).

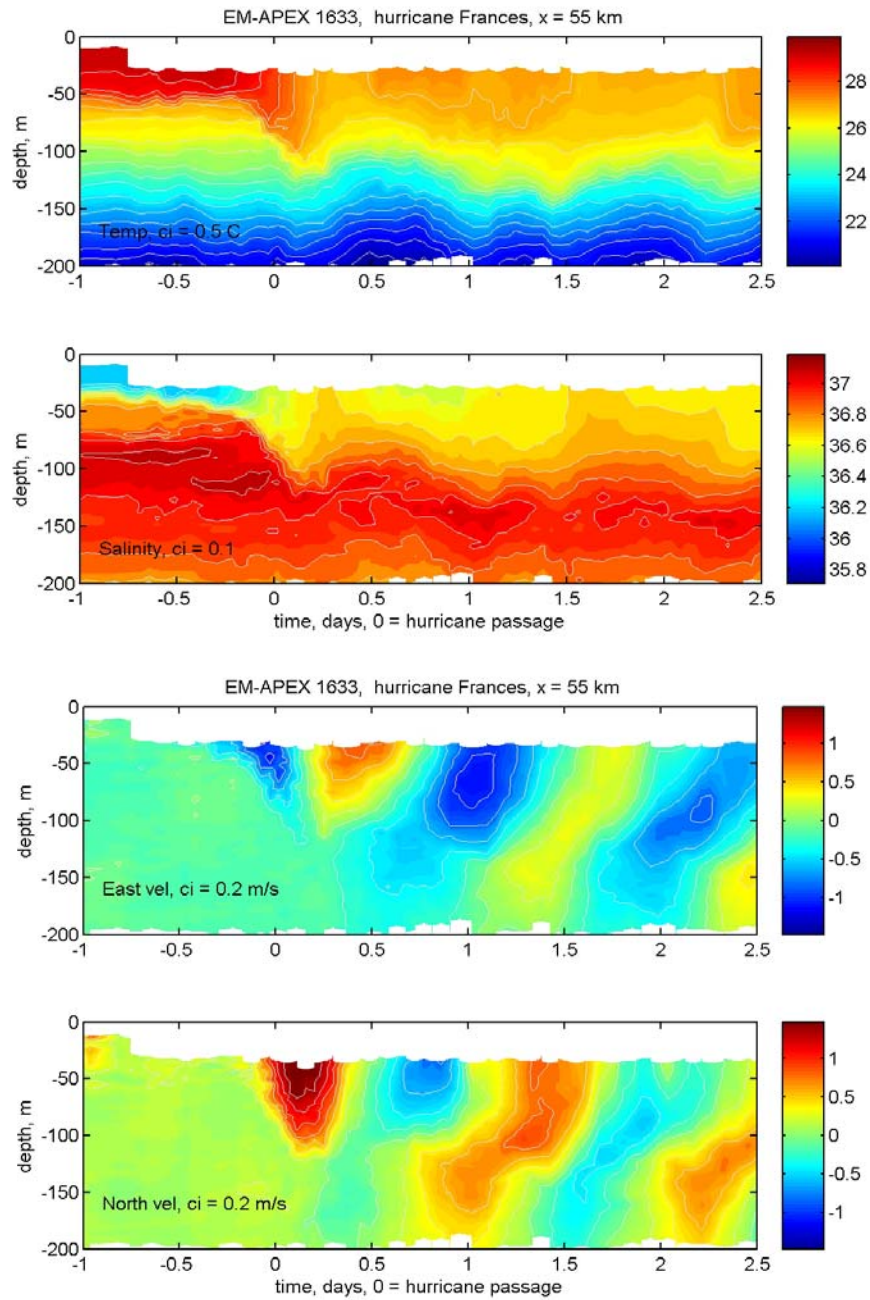


Figure 9. Observed upper-ocean temperature ($^{\circ}\text{C}$) (a), salinity (psu) (b), and current (u, v , in m s^{-1}) (c and d) from the EM-APEX float 1633. Day 0 marks the passage of Hurricane Frances at the float at 1200 UTC on 1 September 2004.

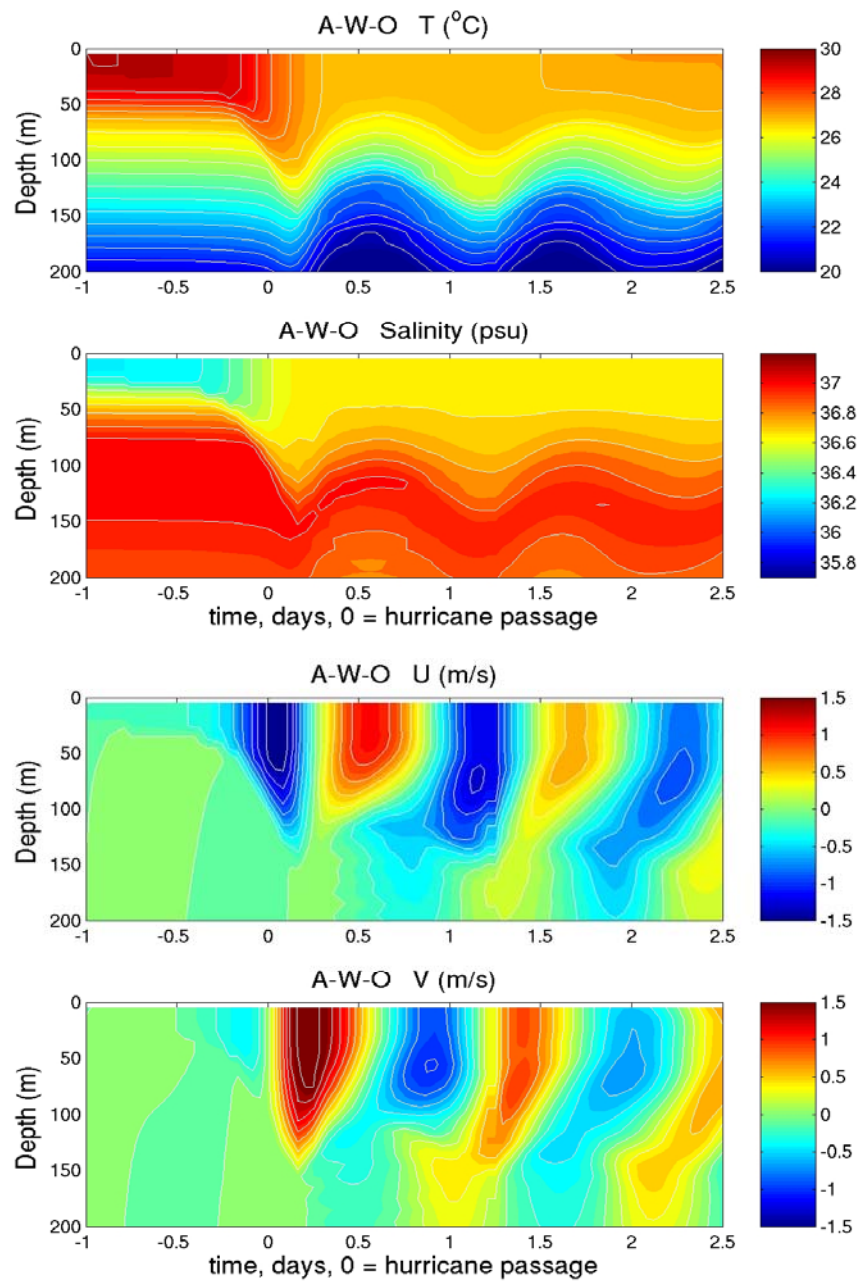


Figure 10. Same as in Fig. 9, except for the fully coupled model simulated fields.

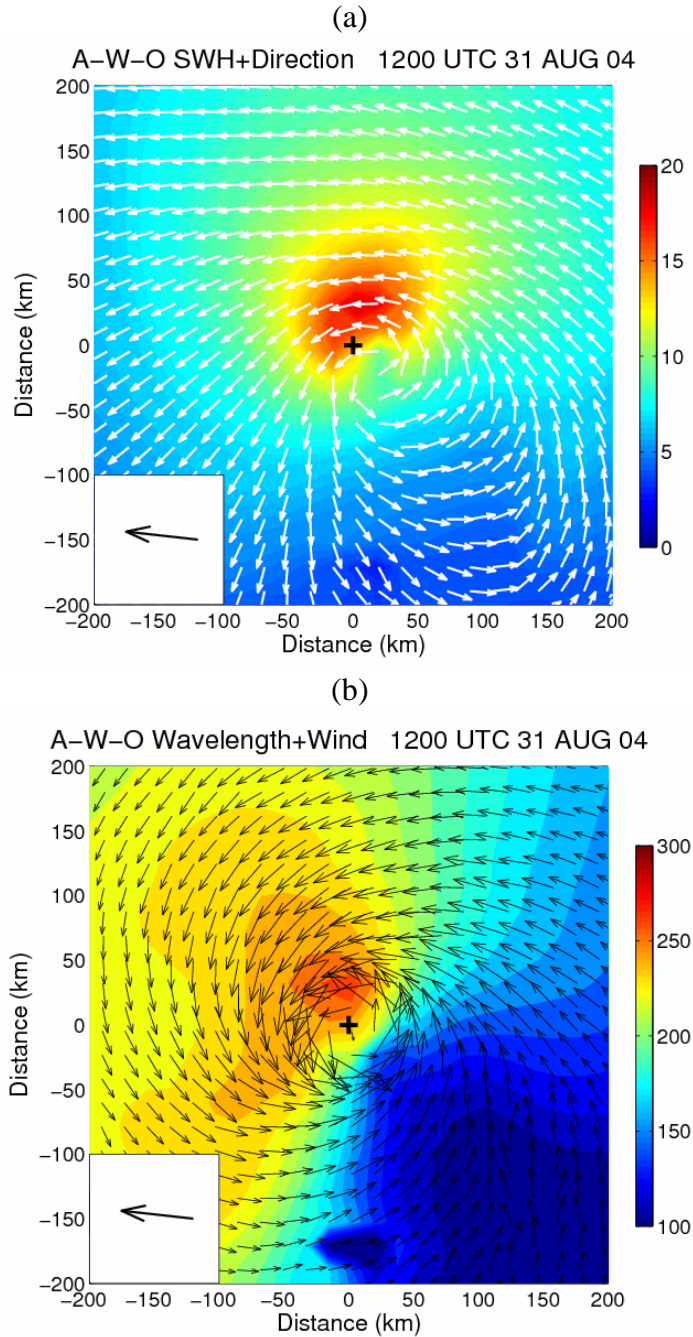


Figure 11. A-W-O model simulated (a) SWH (color, m) and wave propagation direction (white vectors) and (b) mean wavelength (color, m) and surface wind (black vectors) at 1200 UTC on 31 August 2004. The black “+” indicates the storm center of Hurricane Frances. The arrow in the lower left corner indicates the direction of the storm motion.

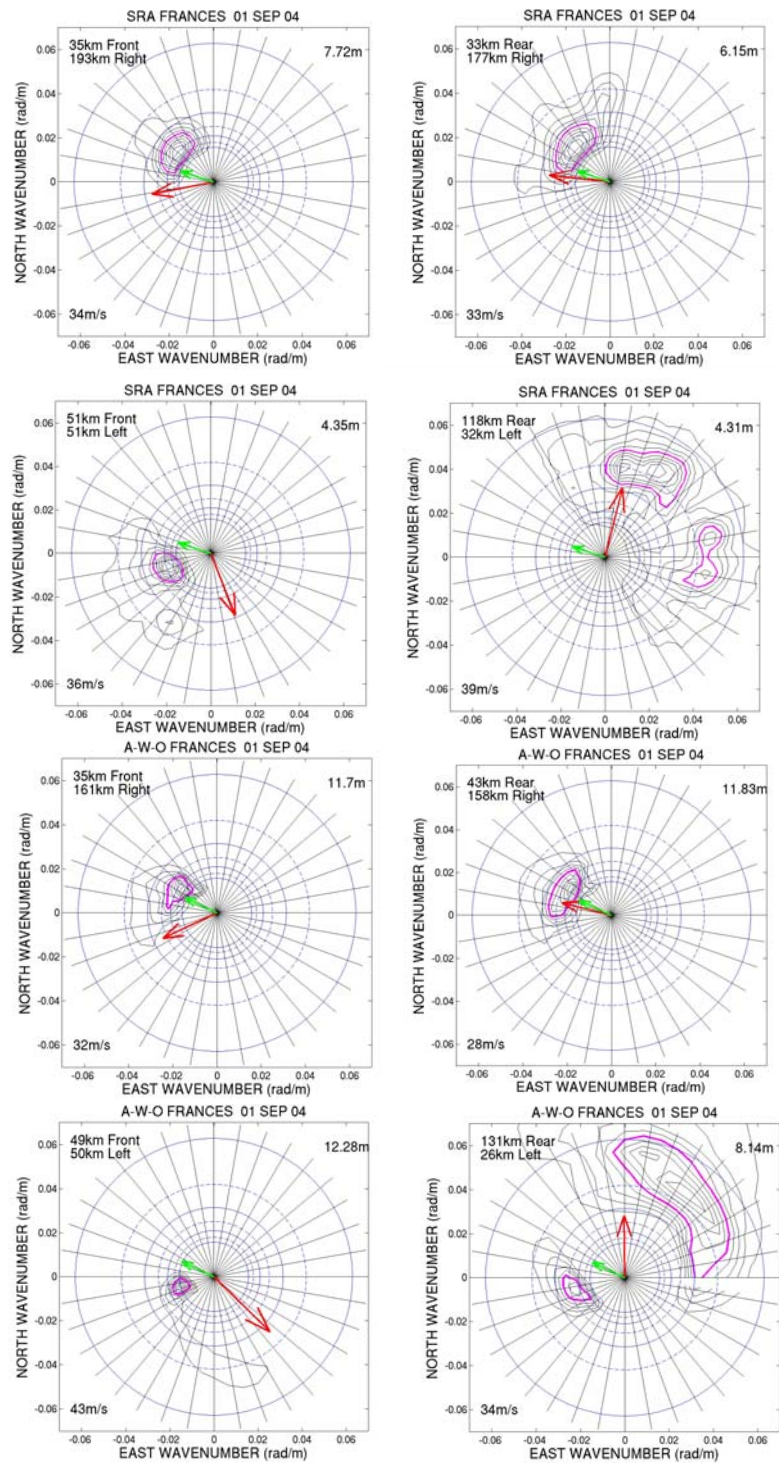


Figure 12. Observed and model simulated directional wave spectra in Hurricane Frances. The top four panels are from the SRA data in the front-left, front-right, rear-left, and rear-right quadrants from 1640-2011 UTC on 1 September 2004. The bottom four panels are the corresponding directional wave spectra from the fully coupled model simulation of Frances.

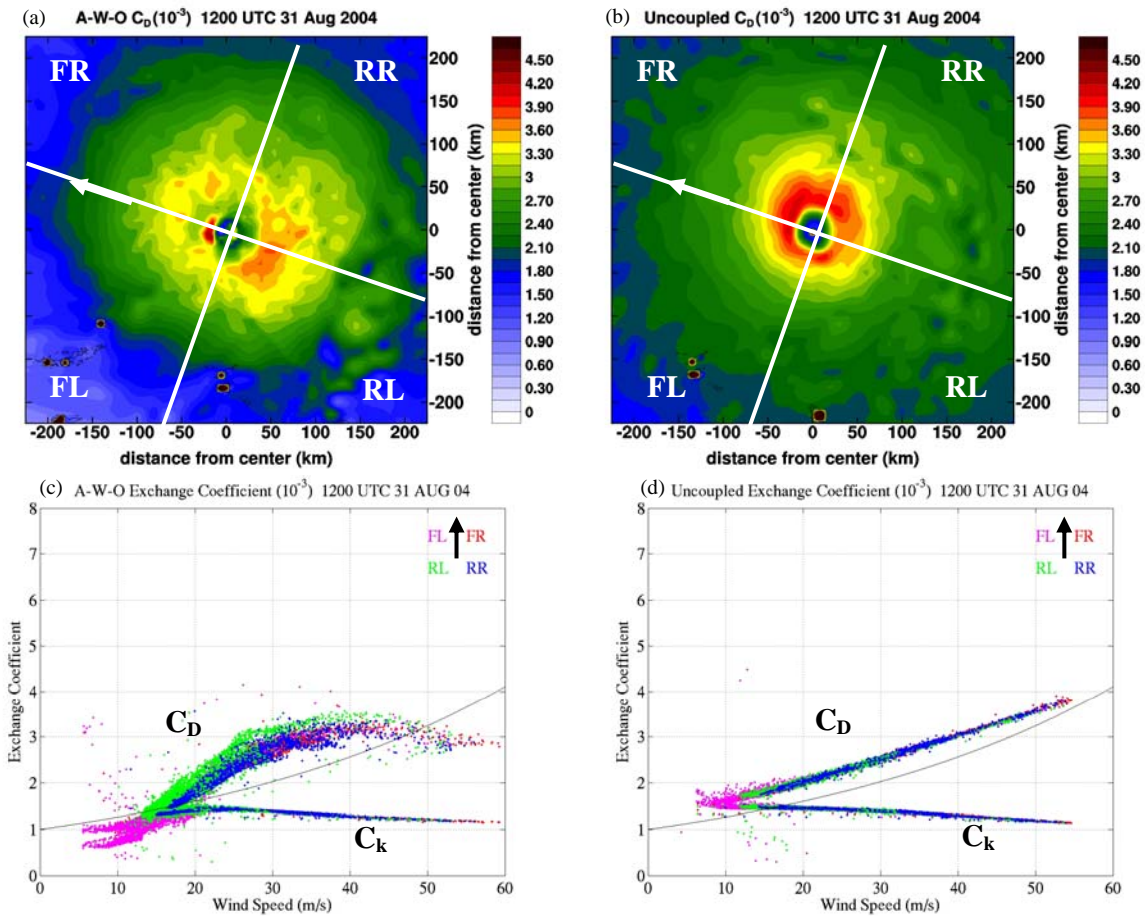


Figure 13. (a) and (b) The fully coupled and uncoupled model simulated drag coefficient in Hurricane Frances at 1200 UTC 31 August 2004. The white lines indicate the four quadrants relative to the storm motion as shown by the white vectors. (c) and (d) Corresponding scatter plots of the drag coefficients and enthalpy exchange coefficient. Data from the four quadrants are shown in different colors as indicated at the top right corner. Similarly the black vectors indicate the direction of the storm motion.

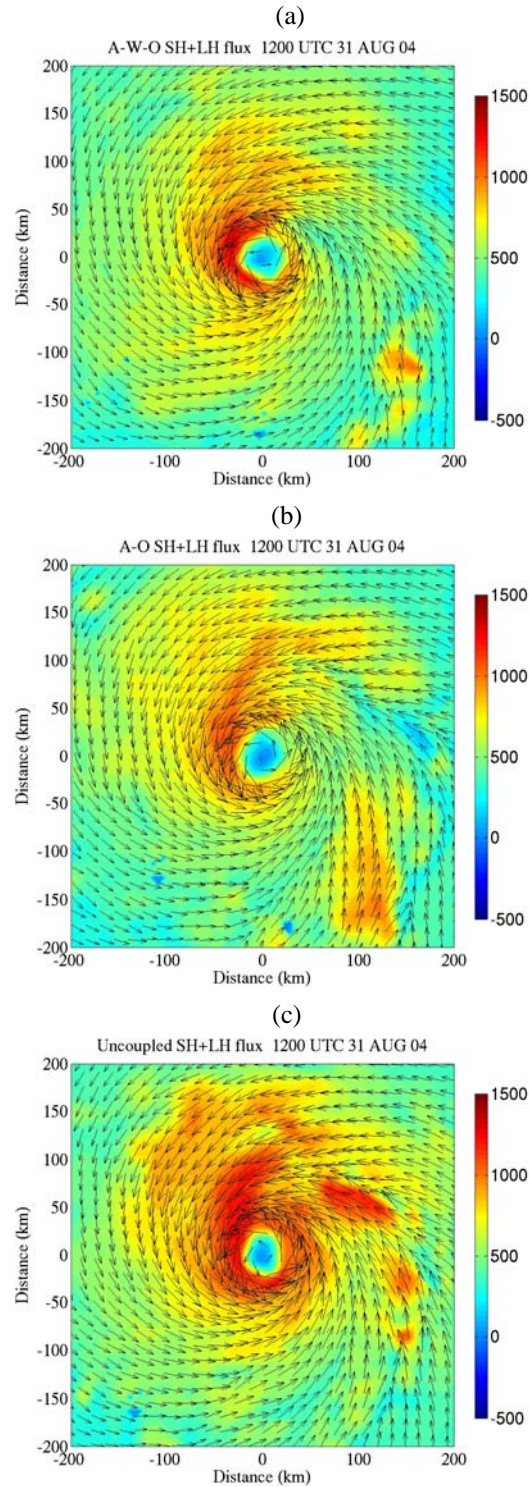


Figure 14. Simulated enthalpy (sensible+latent) flux (color, W m^{-2}) and surface wind (vector) in Hurricane Frances at 1200 UTC 31 August 2004 from (a) fully coupled atmosphere-wave-ocean, (b) coupled atmosphere-ocean, and (c) uncoupled atmosphere models.

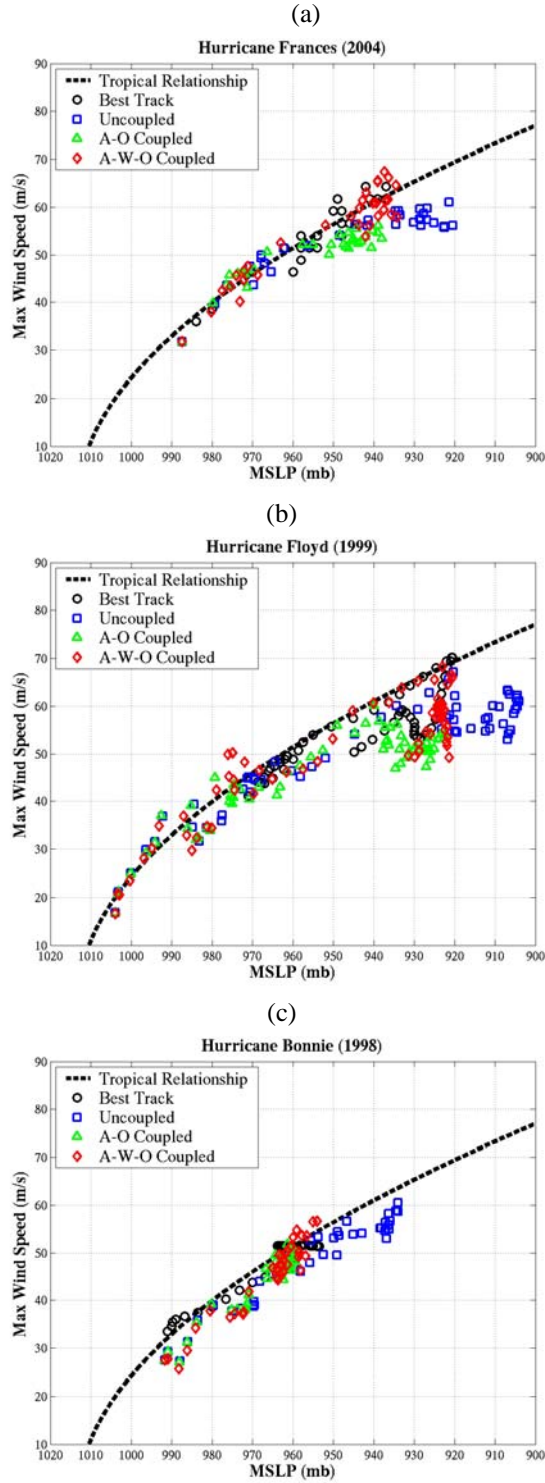


Figure 15. Observed (the NHC best track data, black circles) and simulated pressure-wind relationship from the fully coupled atmosphere-wave-ocean model (red), the coupled atmosphere-ocean model (green), and the uncoupled atmosphere model (blue) for Hurricanes Frances (a), Floyd (b), and Bonnie (c).